Malaysian Journal of Chemistry, 2024, Vol. 26(4), 187-205

Optimisation of Solid-to-Liquid Ratio in *Morinda citrifolia* L. Fruits: Enhancing Yield and Total Flavonoid Content through Extraction Kinetics with High Antioxidant Potential

Mohammad Amil Zulhilmi Benjamin[1], Tun Faiz Al Hakim Tun Faisal Ismail[2] and Mohd Azrie Awang[2,3]*

[1]Borneo Research on Algesia, Inflammation and Neurodegeneration (BRAIN) Group, Faculty of Medicine and Health Sciences, Universiti Malaysia Sabah, Jalan UMS, 88400 Kota Kinabalu, Sabah, Malaysia

[2]Faculty of Food Science and Nutrition, Universiti Malaysia Sabah, Jalan UMS, 88400 Kota Kinabalu, Sabah, Malaysia

[3]Food Security Research Laboratory, Faculty of Food Science and Nutrition, Universiti Malaysia Sabah, Jalan UMS, 88400 Kota Kinabalu, Sabah, Malaysia

*Corresponding author (e-mail: ma.awang@ums.edu.my)

Morinda citrifolia L., commonly known as 'Noni,' holds substantial potential in food and pharmaceutical research due to its bioactive constituents, which can be extracted using innovative techniques. This study specifically focuses on optimising the solid-to-liquid extraction process of crude extracts to obtain yields and total flavonoid content (TFC) from *M. citrifolia* fruits at different solid-to-liquid ratios (1:10 g/mL, 1:20 g/mL, and 1:30 g/mL) using ultrasound-assisted extraction in an ultrasonic water bath. The extraction kinetics were examined using six common mathematical models: first-order kinetic, second-order kinetic, second-order rate, Peleg, power law, and two-site kinetic, along with the assessment of goodness-of-fit. Additional evaluation involved measuring antioxidant activity through the 2,2-diphenyl-1-picrylhydrazyl (DPPH) free radical scavenging assay. The results revealed that at 1:10 and 1:20, the highest yield achieved was 1.46 ± 0.00 mg/mL within 120 min, while the TFC reached 3.57 ± 0.00 mg CE/g db within 110 min, respectively. The two-site kinetic model effectively elucidated the extraction kinetics of both yield and TFC at different ratios, displaying exceptional goodness of fit. For antioxidant activity, the DPPH inhibition results demonstrated significant antioxidant effects, with a peak of 88.39 ± 0.07 % observed at 1:20, compared to the positive control (90.02 ± 0.12 %). Overall, the findings of this study offer valuable insights that contribute to the establishment of standardised extraction methods, cost-effective operations, and time savings for the food and pharmaceutical industries.

Keywords: *Morinda citrifolia*; yield; total flavonoid content; solid-to-liquid ratio; extraction kinetics; antioxidant activity

Received: March 2024; Accepted: June 2024

Extraction kinetics play a vital role in multiple industries, including pharmaceuticals, cosmeceuticals, and nutraceuticals. In the pharmaceutical industry, understanding extraction kinetics is crucial for optimising the extraction of bioactive compounds from medicinal plants, facilitating the efficient production of herbal medicines [1]. Similarly, in the nutraceutical industry, extraction kinetics are essential for improving the extraction of flavour compounds, antioxidants, and other bioactive substances from natural sources, thereby contributing to the development of functional foods and dietary supplements [2]. Additionally, in the cosmeceutical industry, extraction kinetics play a crucial role in extracting plant-derived ingredients such as antioxidants and essential oils, which are valuable for formulating effective and natural beauty products [3]. In scientific research, extraction kinetics are fundamental for understanding dynamic changes, such as the extraction of phytochemicals from plants. This involves using equations such as first-order kinetic, second-order kinetic, second-order rate, Peleg, power law, and two-site kinetic, which are commonly employed in extracting solutes from solid materials [4,5]. These models are essential for fitting experimental data and visualising the extraction process through graph plotting. Optimising extraction processes through an understanding of extraction kinetics is crucial for various industries to efficiently harness the benefits of plant-derived compounds, leading to the development of a wide range of high-quality products with diverse applications.

Morinda citrifolia L., commonly known as 'Noni', has garnered significant interest from scientists due to its numerous benefits [6,7]. This plant is native to Southeast Asia but has spread to different tropical regions such as Australia, Hawaii, and the French Polynesian Islands, possibly through waterborne seed

dispersal or early human migration [6]. This migration had led to the widespread occurrence of this species in the Indo-Pacific Islands, influenced by the migratory routes of seafaring Polynesians. Different parts of the *M. citrifolia* plant, such as the leaves, fruits, roots, and seeds, have been scientifically explored for their culinary and medicinal applications [7]. Abou Assi et al. [8] extensively outlined various pharmacological effects attributed to *M. citrifolia*, including antioxidant, anti-inflammatory, antibacterial, antifungal, antiviral, antitumour, anthelminthic, analgesic, hypotensive, and immune-enhancing effects. Since the 1990s, these characteristics have been utilised for commercial purposes in America. Additionally, the fruit juice of *M. citrifolia* was authorised as a Novel Food by the European Commission in 2010 [9]. This authorisation signifies *M. citrifolia* as a prominent global food source, owing to its nutritional and therapeutic properties.

Flavonoids comprise natural substances characterised by various phenolic structures found in different sources such as fruits, vegetables, tea, wine, bark, flowers, grains, roots, and stems [10]. Bioactive compounds like coumarins and anthraquinones have been observed in *M. citrifolia* root extracts along with flavonoids, showcasing diverse biological activities including antioxidant, anti-inflammatory, antibacterial, antifungal, and antiviral properties [11]. Several studies have reported the presence of additional chemical constituents such as anthraquinones (and their glycosides), tannins (and their derivatives), iridoids (secoiridioid glucosides and acetates), sterols [stigmasterol (**1**) and β-sitosterol (**2**)], amino acids [proline (**3**)], fatty acids [linoleic acid (**4**)], lignans [dehydrodiisoeugenol (**5**)], polysaccharides (pectin), and sugars occurring predominantly as monosaccharides or

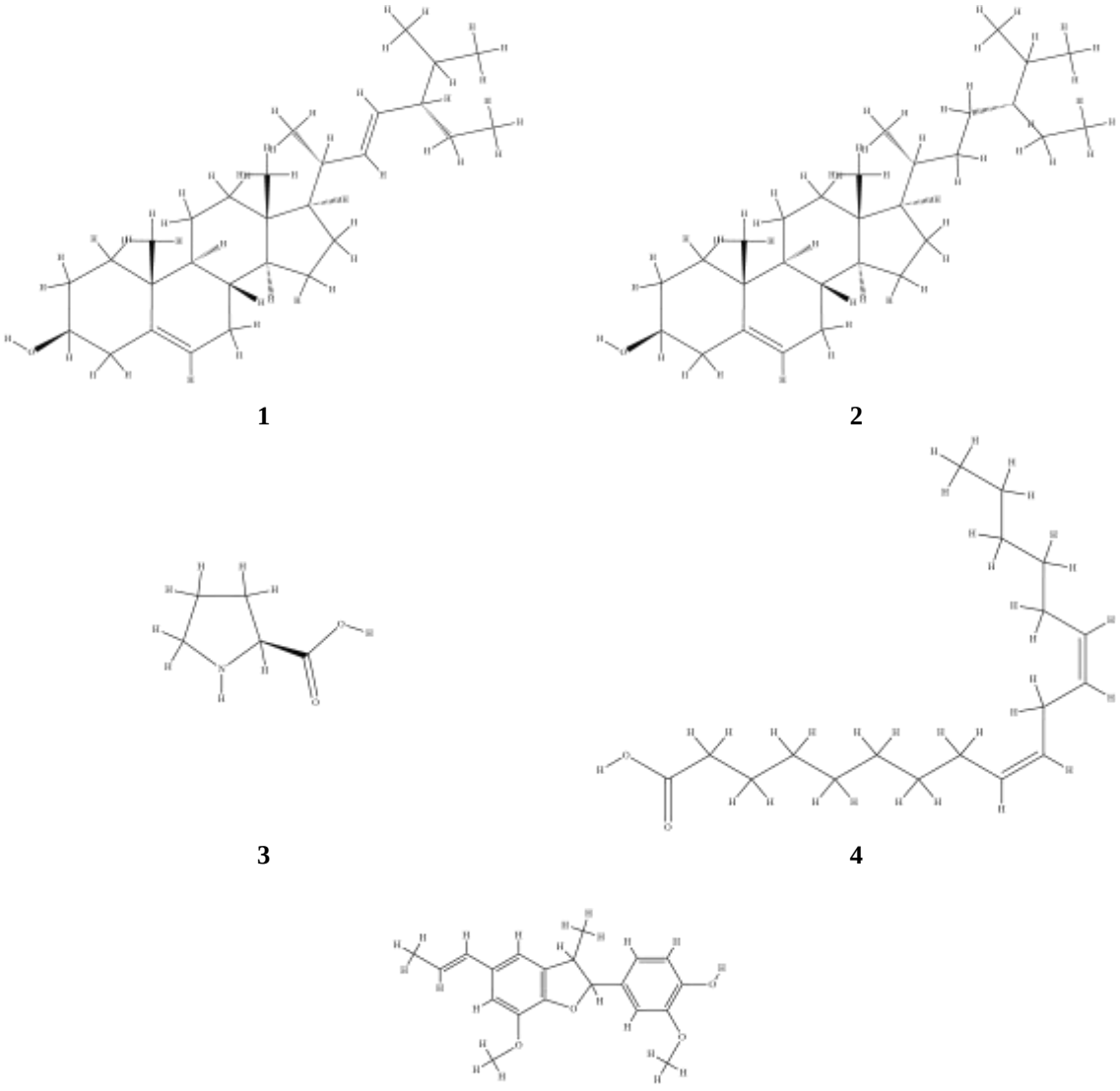

1 **2** **3** **4** **5**

Figure 1. Structures of major compounds in *M. citrifolia*.

oligosaccharides in crude extracts obtained from various plant parts and fruit juice [12]. The structures of major compounds (**1**–**5**) in *M. citrifolia* are depicted in Figure 1. A comprehensive study on *M. citrifolia* highlighted the presence of flavonoids among the array of biochemically active compounds in this species [7].

Despite the potential therapeutic benefits of *M. citrifolia* fruits, the scientific inquiry into their extraction kinetics faces significant knowledge gaps. This has resulted in inefficient extraction methods and the absence of standardised procedures in the industry. Inadequate research on extraction kinetics, particularly regarding ratios, has led to a lack of standard methods, increasing costs and time requirements for industry stakeholders. Therefore, this study aims to leverage mathematical modelling as an effective engineering tool to comprehend the extraction kinetics of both yield and total flavonoid content (TFC) from crude extracts of *M. citrifolia* fruits across various solid-to-liquid ratios. By addressing these knowledge gaps, this study aims to provide valuable insights that contribute to the development of standardised extraction methods.

EXPERIMENTAL

Sample Preparation

A batch of 2 kg of fully mature and ripe *M. citrifolia* fruits was procured from Universiti Malaysia Sabah, Sabah, Malaysia (Coordinates: 6°02'16.4" N 116°07'38.8" E). The fruits underwent thorough rinsing with tap water to remove any foreign particles from their surface. Subsequently, the seeds were extracted, and the pulp was hand-cut using a stainless-steel knife. A convection drying oven (ED 23, Binder, Neckarsulm, Germany) was pre-set to a drying temperature of 60 °C, and the samples were dried until a consistent weight was achieved. Once dried, the samples were finely ground into a powder using a grinder (EBM-9182, Elba, Borso del Grappa, Italy). This powdered sample was carefully sealed for subsequent analysis.

Extraction Procedure

In this experiment, 10 g of the ground sample were precisely measured and mixed with 99.8 % absolute ethanol in a conical flask at a solid-to-liquid ratio of 1:10 g/mL (w/v) for extraction, following the procedure outlined by Stephenus et al. [13]. Ultrasound-assisted extraction was initiated using a sonication water bath (CPX8800H, Branson, Brookfield, CT, USA) set at a frequency of 37 kHz and 70 W power input. The extraction process was carried out at 50 °C with intermittent swirling every 10 min over a 120-minute period. The same procedure was repeated for two additional ratios, 1:20 and 1:30. Subsequently, the samples underwent filtration using Whatman No. 1 filter paper (Maidstone, Kent, UK). The obtained filtrates were processed using a rotary evaporator (Laborota 4000, Heidolph, Schwabach, Germany) until crude extracts were obtained. These crude extracts were then dried using a convection drying oven to eliminate any remaining solvent. The extraction yield of the sample was evaluated following the procedure outlined by Lin et al. [14] with minor adjustments. The evaporated dried extract was weighed using a digital balance (ADB 100-4, Kern & Sohn GmbH, Balingen, Germany). The concentration-based yield was determined using Equation (1):

$$C_a = \frac{m}{V} \quad (1)$$

where C_a is the concentration of the crude extract (mg/mL), m is the weight of the dried extract (mg), and V is the volume of the solvent used for extraction (mL).

Total Flavonoid Content

The TFC of the sample was determined using an aluminium colorimetric assay following the procedure outlined by Awang et al. [15] and Hobbi et al. [16] with some modifications. Initially, 1 mL of crude extract was mixed with 1 mL of 10 % aluminium chloride, and the resulting mixture was incubated in the dark for 15 min at room temperature. Subsequently, the absorbance of the solution was measured at 510 nm using an ultraviolet–visible spectrophotometer (Lambda 25, Perkin Elmer, Waltham, MA, USA). TFC was quantified in milligrams of catechin equivalent per gram on a dry basis (mg CE/g db), employing catechin as the standard reference based on the calibration curve (y = 0.0589x – 0.0277). Equation (2) was utilised to calculate the TFC of the crude extract:

$$\text{Concentration of TFC (mg CE/g db)} = \frac{C_b \times V}{m} \quad (2)$$

where C_b is the concentration of the crude extract (mg/mL) obtained from the TFC standard curve.

Extraction Kinetics Models

1. First-order Kinetic Model

The first-order kinetic model was selected because the mass balance of yield for a unit of liquid volume during extraction [17] can be represented by Equation (3):

$$\frac{dC_t}{dt} = -k \cdot (C_s - C_t) \quad (3)$$

Integrating Equation (4) to determine the kinetic parameters involves applying the following boundary conditions: from $C_t = 0$ to C_t and from t = 0 to t, leading to the outcome expressed by Equation (5):

$$\int_0^{C_t} \frac{dC_t}{C_s - C_t} = -k \int_0^t dt \quad (4)$$

$$C_t = C_s \cdot (1 - e^{-k \cdot t}) \quad (5)$$

where C_t is the concentration of the yield (mg/mL) or TFC (mg CE/g db) obtained from the crude extract at a specific time t (min), C_s is the concentration of the yield (mg/mL) or TFC (mg CE/g db) at the saturation point, and k is the first-order rate constant (min^{-1}).

2. Second-order Kinetic Model

For the second-order kinetic model, Equation (6) describes the mass balance of the product yield for a unitary liquid volume during extraction [16].

$$\frac{dC_t}{dt} = k \cdot (C_s - C_t)^2 \quad (6)$$

To obtain the kinetic parameters by integrating Equation (7), the following boundary conditions are applied: from $C_t = 0$ to C_t and from t = 0 to t, resulting in Equation (8):

$$\int_0^{C_t} \frac{dC_t}{(C_s - C_t)^2} = k \int_0^t dt \quad (7)$$

$$C_t = \frac{C_s^{\,2} \cdot k \cdot t}{1 + C_s \cdot k \cdot t} \quad (8)$$

where k is the second-order rate constant (min^{-1}).

3. Second-order Rate Model

The second-order rate model offers a satisfactory explanation for the solid-to-liquid extraction process [5,18]. Therefore, this model was employed to illustrate the kinetics of the yield and TFC. Equation (8), derived from the second-order kinetic model, delineates the dissolution rate of extractable substances. Upon rearrangement, the concentration of extractable substances at any given time can be expressed by Equation (9):

$$C_t = \frac{1}{(1/h) + (t/C_s)} \quad (9)$$

where h is the initial extraction rate of the yield (mg/mL·min) or TFC (mg CE/g db·min).

4. Peleg Model

The model initially proposed by Peleg [19] to depict sorption curves was modified to characterise the solid-to-liquid extraction process, employing Equation (10):

$$C_t = C_0 + \frac{t}{k_1 + k_2 \cdot t} \quad (10)$$

where k_1 represents Peleg's rate constant of the yield (mL·min/mg) or TFC (g db·min/mg CE), k_2 represents Peleg's capacity constant of the yield (mL/mg) or TFC (g db/mg CE), and C_0 represents the concentration of the yield (mg/mL) or TFC (mg CE/g db) at time t = 0. k_1 is related to the extraction rate at the initial stage of the extraction process, whereas k_2 is related to the peak extraction rate throughout the extraction process. At t = 0, $C_0 = 0$. Consequently, Equation (11) underwent modification and took the following form:

$$C_t = \frac{t}{k_1 + k_2 \cdot t} \quad (11)$$

5. Power Law Model

The power law model has been utilised to elucidate the extraction process in solid-to-liquid extraction [20]. It can be expressed by Equation (12):

$$C_t = B \cdot t^n \quad (12)$$

where B is the constant related to the extraction rate of the yield (mg/mL·min) or TFC (mg CE/g db·min), and n represents the diffusional exponent which must be < 1 when extracting from plant cells.

6. Two-site Kinetic Model

A widely recognised two-site kinetic model, introduced by So and MacDonald [21], is commonly employed to describe the extraction process. According to this model, the extraction process consists of two stages: washing and diffusion. During the washing stage, the solute is rapidly removed from external surfaces and cracks, while in the diffusion stage, solute transfer occurs through interior parts via internal diffusion. This model can be represented by Equation (13).

where C_w and C_d represent the concentrations of the yield (mg/mL) or TFC (mg CE/g db) recovered during the washing and diffusion stages, respectively, and k_w and k_d represent the extraction rate coefficients of the yield (mL/mg·min) or TFC (g db/mg CE·min) during the washing and diffusion stages, respectively.

$$C_t = C_w \cdot \left[1 - e^{(-k_w \cdot t)}\right] + C_d \cdot \left[1 - e^{(-k_d \cdot t)}\right] \quad (13)$$

Goodness of Fit

Statistical tools were used to compare and evaluate the goodness of fit for various models selected to determine the best mathematical model for assessing the yield and TFC data in *M. citrolia* fruits based on their ratios. The statistical metrics utilised in this analysis include the coefficient of determination (R^2), adjusted coefficient of determination (R^2_{adj}), root mean square error (RMSE), chi-square (χ^2), and mean absolute error (MAE), which are defined by Equations (14), (15), (16), (17), and (18), respectively.

where k is the number of independent variables, N is the total number of data points, n is the number of observations, y_i is the observed value, $\hat{y}_i$ is the predicted value, and $\bar{y}$ is the mean of the actual values.

Antioxidant Analysis

The 2,2-diphenyl-1-picrylhydrazyl (DPPH) free radical scavenging assay was performed according to the method outlined by Awang et al. [22], with minor adjustments. In brief, 1 mL of the crude extract was mixed with 1 mL of a methanolic solution containing DPPH (0.1 mM). The resulting mixture was incubated in the dark at room temperature for 30 min. After incubation, the absorbance was measured spectrophotometrically at 517 nm against a blank. Ascorbic acid was utilised as the positive control. The free radical scavenging activity of the extract against DPPH was determined using Equation (19).

where A_c and A_s are the control and sample absorbances, respectively.

Statistical Analysis

All experiments were conducted in triplicate, and the results are reported as mean ± standard deviation. Yield and TFC data were analysed using one-way analysis of variance (ANOVA) and Tukey's Honestly Significant Difference (HSD) tests, with the significance set at $p < 0.05$. Statistical analysis was performed using SPSS (Version 28). Microsoft Office 2019 (Excel Solver) was employed to model extraction kinetics. The compounds were validated in PubChem, and their compound structures were depicted using ChemDraw Ultra (Version 12).

$$R^2 = 1 - \left[\frac{\sum_{i=1}^{n}\left(y_i - \hat{y}_i\right)^2}{\sum_{i=1}^{n}\left(y_i - \bar{y}\right)^2}\right] \tag{14}$$

$$R^2_{adj} = 1 - \frac{\left(1 - R^2\right) \times (n - 1)}{n - k - 1} \tag{15}$$

$$RMSE = \sqrt{\frac{\sum_{i=1}^{n}\left(y_i - \hat{y}_i\right)^2}{n}} \tag{16}$$

$$\chi^2 = \sum_{i=1}^{n} \frac{\left(y_i - \hat{y}_i\right)^2}{\hat{y}_i} \tag{17}$$

$$MAE = \frac{1}{N}\sum_{i=1}^{n} \left|y_i - \hat{y}_i\right| \tag{18}$$

$$\text{DPPH free radical scavenging activity (\%)} = \frac{A_c - A_s}{A_c} \times 100 \tag{19}$$

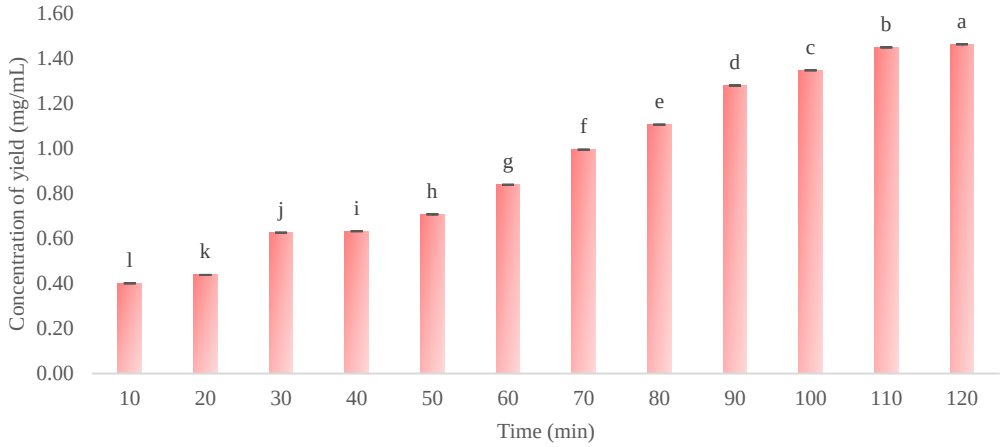

1:10

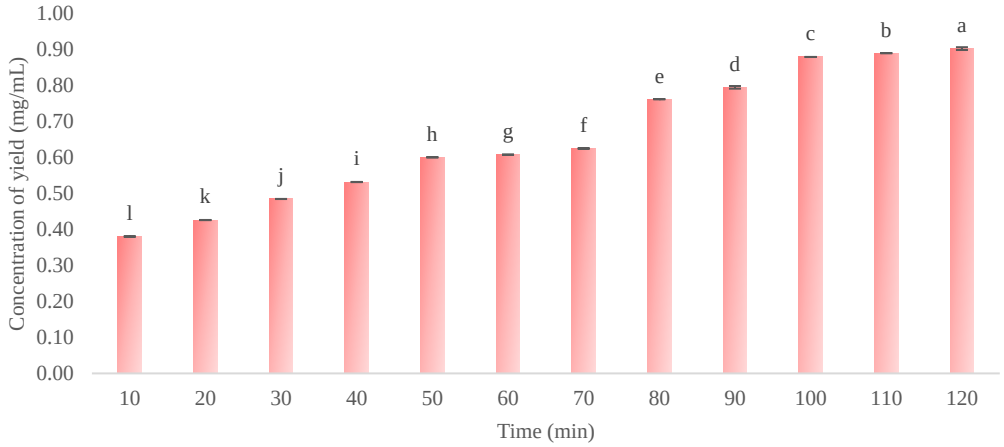

1:20

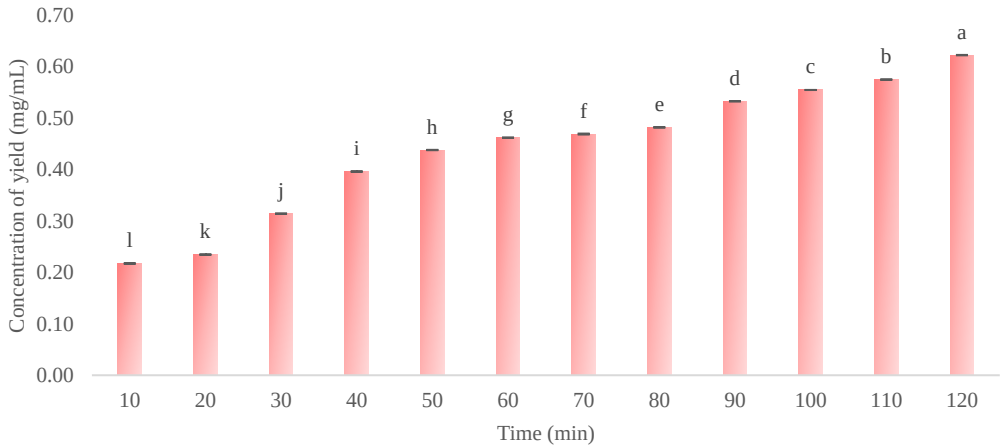

1:30

Figure 2. Concentrations of the yields in *M. citrifolia* fruits at different solid-to-liquid ratios over time. Values signify means ± standard deviations of three replicates. Distinct letters (within a bar) denote statistically significant differences (one-way ANOVA, Tukey's HSD test, $p < 0.05$).

RESULTS

Effect of Solid-to-Liquid Ratios on Extraction Kinetics of Yield

Figure 2 illustrates the experimental results depicting the yields from *M. citrifolia* fruits at different solid-to-liquid ratios of 1:10, 1:20, and 1:30 over a 0 to 120-minute period. The findings demonstrate a gradual increase in yields for all ratios within the 120-minute timeframe. Specifically, at 1:10, the yield reached 1.46 ± 0.00 mg/mL within 120 min. Similarly, at 1:20 and 1:30, the highest yield values were 0.90 ± 0.00 mg/mL and 0.62 ± 0.00 mg/mL, respectively, all within the 120-minute duration. These results highlight the significant impact of varying ratios on the yield, as indicated by noteworthy differences ($p < 0.05$) among the values. Furthermore, the results suggest an initial decrease in the yield under all conditions within the initial 10 min, followed by a gradual increase. The 1:10 exerted a more pronounced influence on the yield for *M. citrifolia* fruits compared to 1:20 and 1:30.

Six mathematical models, namely the first-order kinetic, second-order kinetic, second-order rate, Peleg, power law, and two-site kinetic models, were applied to assess the extraction kinetics of the yield for *M. citrifolia* fruits across different ratios, as depicted in Figure 3. This comparison between experimental and predicted extraction kinetics models was based on various solid-to-liquid ratios for *M. citrifolia* fruits. The model with the highest R^2 and R^2_{adj} values, coupled with the lowest RMSE, χ^2, and MAE values, was selected to determine the goodness of fit. The results are summarised in Table 1, showing R^2 values ranging from 0.920 to 0.969 for the first-order kinetic model, 0.935 to 0.978 for the second-order kinetic model, 0.864 to 0.970 for the second-order rate model, 0.935 to 0.978 for the Peleg model, 0.974 to 0.987 for the power law model, and 0.987 to 0.989 for the two-site kinetic model. Additionally, R^2_{adj} values ranged from 0.011 to 0.066 for the first-order kinetic model, 0.029 to 0.075 for the second-order kinetic model, –0.050 to 0.067 for the second-order rate model, 0.029 to 0.075 for the Peleg model, 0.071 to 0.086 for the power law model, and 0.086 to 0.088 for the two-site kinetic model. RMSE values varied from 0.513×10^{-3} to 3.618×10^{-3} for the first-order kinetic model, 0.351×10^{-3} to 3.456×10^{-3} for the second-order kinetic model, 1.827×10^{-3} to 3.590×10^{-3} for the second-order rate model, 0.351×10^{-3} to 3.456×10^{-3} for the Peleg model, 0.189×10^{-3} to 2.160×10^{-3} for the power law model, and 0.189×10^{-3} to 1.124×10^{-3} for the two-site kinetic law model. Another critical parameter to determine the validity of the models is χ^2. The lowest χ^2 values ranged from 0.898×10^{-4} to 3.553×10^{-4} for the first-order kinetic model, 0.236×10^{-4} to 2.555×10^{-4} for the second-order kinetic model, 0.000×10^{-4} for the second-order rate model, 0.236×10^{-4} to 2.556×10^{-4} for the Peleg model, 0.000×10^{-4} to 0.298×10^{-4} for the power law model, and 0.000×10^{-4} for the two-site kinetic model. Lastly, MAE values were observed from 0.386×10^{-2} to 1.589×10^{-2} for the first-order kinetic model, 0.198×10^{-2} to 1.388×10^{-2} for the second-order kinetic model, 0.000×10^{-2} for the second-order rate model, 0.198×10^{-2} to 1.388×10^{-2} for the Peleg model, 0.001×10^{-2} to 0.474×10^{-2} for the power law model, and 0.000×10^{-2} for the two-site kinetic model.

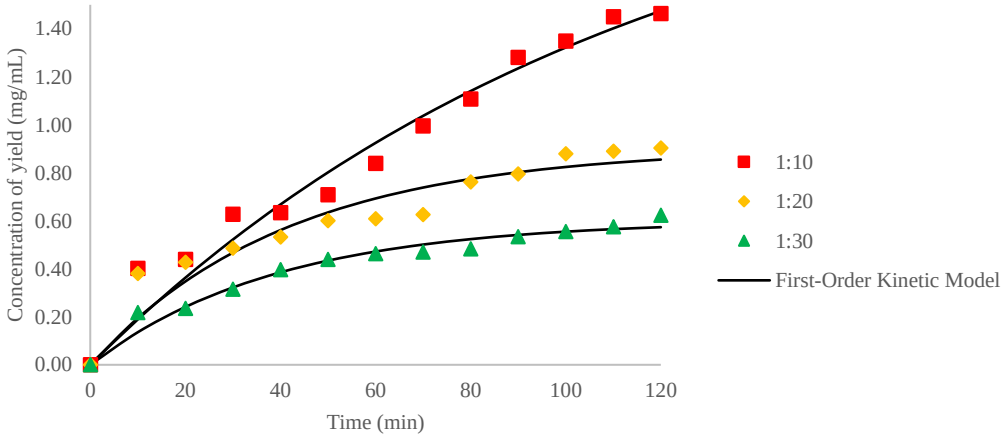

First-order kinetic

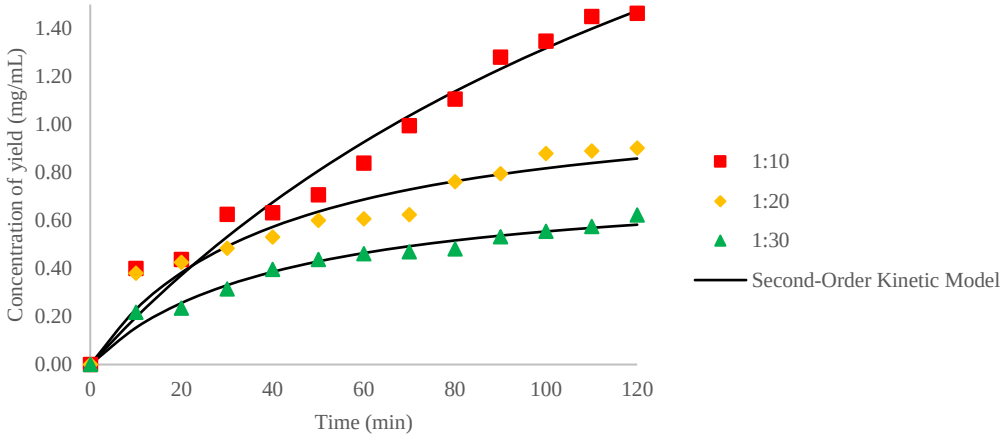

Second-order kinetic

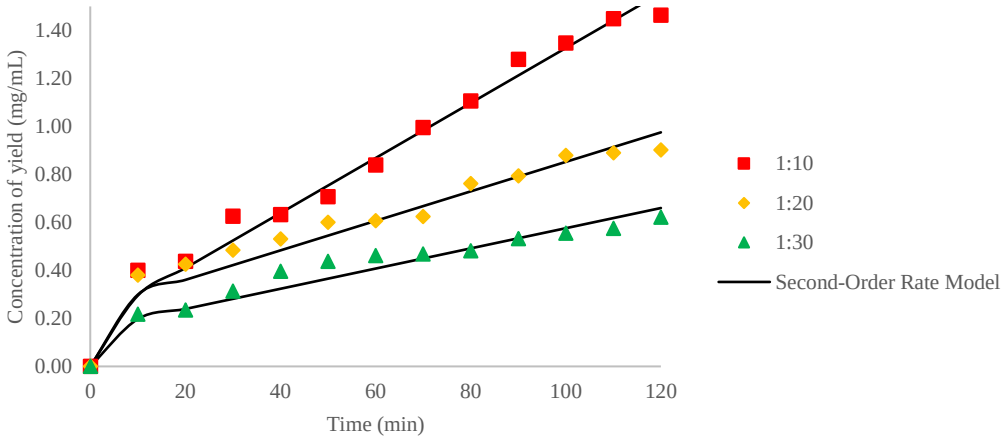

Second-order rate

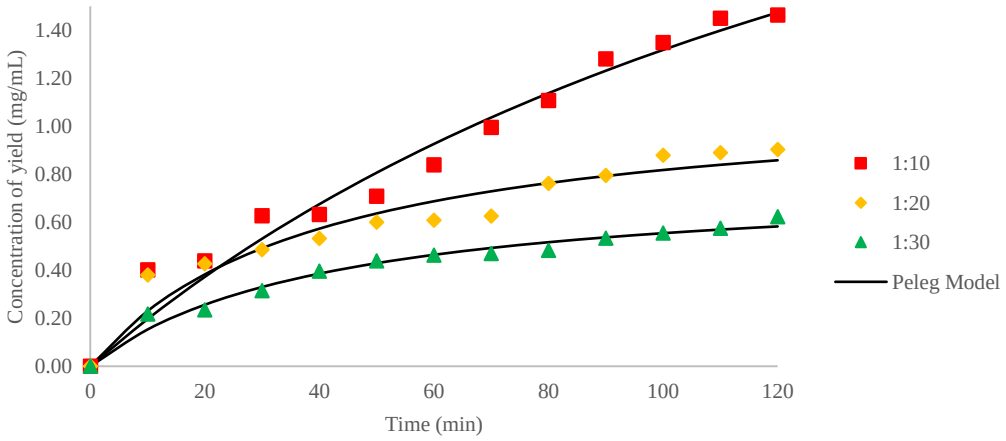

Peleg

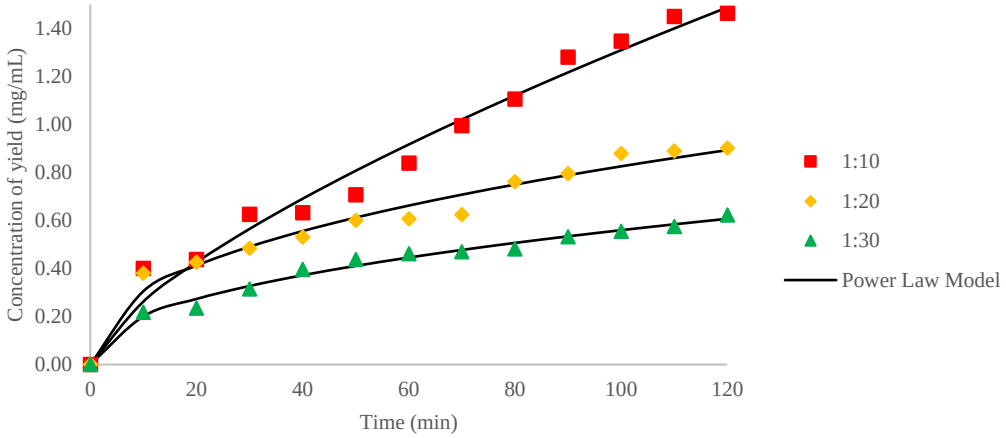

Power law

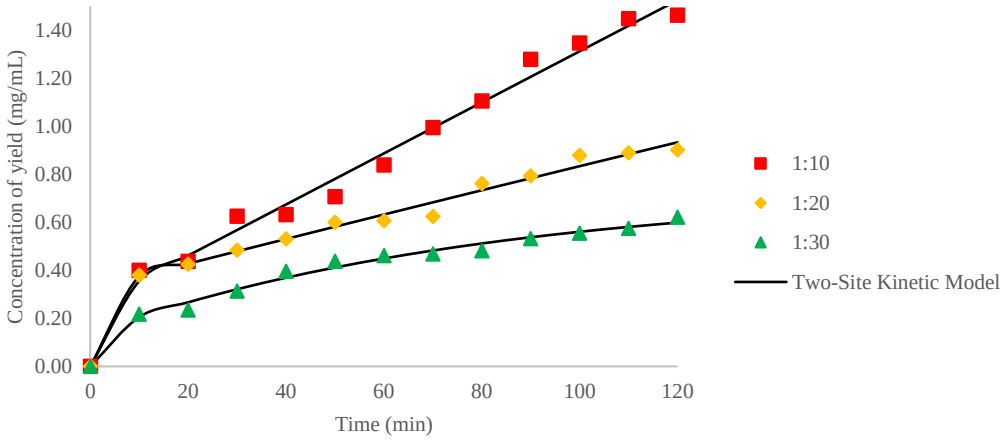

Two-site kinetic

Figure 3. Comparison of experimental and predicted data for the extraction kinetics models for the yield of *M. citrifolia* fruits at different solid-to-liquid ratios.

Table 1. Goodness of fit analysis for extraction kinetics models for the yield of *M. citrifolia* fruits at different solid-to-liquid ratios.

Model	Ratio	Constant		R^2	R^2_{adj}	RMSE (10^{-3})	χ^2 (10^{-4})	MAE (10^{-2})
First-order kinetic	1:10	C_e =	2.284	0.968	0.065	3.618	3.349	1.589
		k =	0.009					
	1:20	C_e =	0.905	0.920	0.011	2.961	3.553	1.143
		k =	0.024					
	1:30	C_e =	0.601	0.969	0.066	0.513	0.898	0.386
		k =	0.026					
Second-order kinetic	1:10	C_s =	3.607	0.969	0.066	3.456	2.555	1.388
		k =	0.002					
	1:20	C_s =	1.142	0.935	0.029	2.211	1.038	0.618
		k =	0.022					
	1:30	C_s =	0.782	0.978	0.075	0.351	0.236	0.198
		k =	0.031					
Second-order rate	1:10	h =	0.181	0.970	0.067	2.996	0.000	0.000
		C_s =	87.253					
	1:20	h =	0.238	0.875	–0.038	3.590	0.000	0.000
		C_s =	162.677					
	1:30	h =	0.155	0.864	–0.050	1.827	0.000	0.000
		C_s =	237.751					

Peleg	1:10	k_1 =	48.133	0.969	0.066	3.456	2.556	1.388
		k_2 =	0.277					
	1:20	k_1 =	34.763	0.935	0.029	2.211	1.038	0.618
		k_2 =	0.875					
	1:30	k_1 =	52.495	0.978	0.075	0.351	0.236	0.198
		k_2 =	1.279					
Power law	1:10	B =	0.052	0.979	0.077	2.160	0.298	0.474
		n =	0.699					
	1:20	B =	0.113	0.974	0.071	0.850	0.049	0.134
		n =	0.432					
	1:30	B =	0.072	0.987	0.086	0.189	0.000	0.001
		n =	0.446					
Two-site kinetic	1:10	C_w =	1657.762	0.989	0.088	1.124	0.000	0.000
		k_w =	0.000					
		C_d =	0.000					
		k_d =	89.414					
	1:20	C_w =	12.527	0.989	0.088	0.349	0.000	0.000
		k_w =	0.000					
		C_d =	0.026					
		k_d =	16.553					
	1:30	C_w =	0.600	0.987	0.086	0.189	0.000	0.000
		k_w =	0.012					
		C_d =	0.226					
		k_d =	1.882					

The two-site kinetic model demonstrated the highest R^2 value for both 1:10 and 1:20 (0.989), but was slightly lower at 1:30 (0.987), with similar trends observed in the R^2_{adj} values. Additionally, the RMSE, χ^2, and MAE values were lower for the two-site kinetic model compared to other models. Considering these metrics, the two-site kinetic model emerges as a promising choice for characterising the yield extraction kinetics for *M. citrifolia* fruits across all ratios, given its exceptional fit. Extraction rate coefficients (k_w and k_d) and the concentrations of the recovered yield (C_w and C_d) provide insights into the efficiency of the extraction process. Notably, C_w values sharply decreased from 1657.762 mg/mL at 1:10 to 0.600 mg/mL at 1:30, indicating lower yield recoveries with higher ratios during the washing stage. Conversely, C_d values increased from 0.000 mg/mL at 1:10 to 0.226 mg/mL at 1:30, indicating higher yields in the diffusion stage with higher ratios. These changes were inferred based on the gradual removal of the target solute from the solid matrix, occurring at a slower rate during the washing stages and at a faster rate during the diffusion stages, as the ratios increased, affecting the yields for *M. citrifolia* fruits.

Furthermore, k_w values indicate a very low extraction rate during the washing stage, with a slight increase from 0.000 mL/mg·min at 1:10 to 0.012 mL/mg·min at 1:30, while k_d values decreased significantly from 89.414 mL/mg·min at 1:10 to 1.882 mL/mg·min at 1:30, indicating a reduced extraction rate during the diffusion stage as the ratio increased. A steady increase in the extraction rate of k_w as the ratios increased implies that extraction carried out at 1:30 provided the fastest yield of the quickly released solutes in the very early part of the extraction. However, a decrease in the extraction rate of k_d as the ratios increased suggests the slowest yield extraction as the quickly released fractions occurred. These parameters highlight how the extraction process efficiency correlated with ratio changes, offering crucial insights for optimising both yield and efficiency.

Effect of Solid-to-Liquid Ratios on Extraction Kinetics of TFC

Figure 4 depicts the outcomes of the experiment conducted on *M. citrifolia* fruits across different ratios of 1:10, 1:20, and 1:30 over a 120-minute duration. Specifically, at a 1:10, the peak TFC value of 3.46 ± 0.02 mg CE/g db was achieved within 100 min. For 1:20, the highest TFC value occurred at 110 min (3.57 ± 0.00 mg CE/g db), while at 1:30, the maximum TFC value was 3.19 ± 0.00 mg CE/g db, obtained between 110 and 120 min. These results highlight the substantial impact of varying ratios on TFC, with significant differences ($p < 0.05$) observed among the values. Additionally, there was an initial decrease in TFC across all conditions within the first 10 min, followed by a gradual increase. Notably, the 1:20 had a stronger influence on higher TFC value compared to both 1:10 and 1:30.

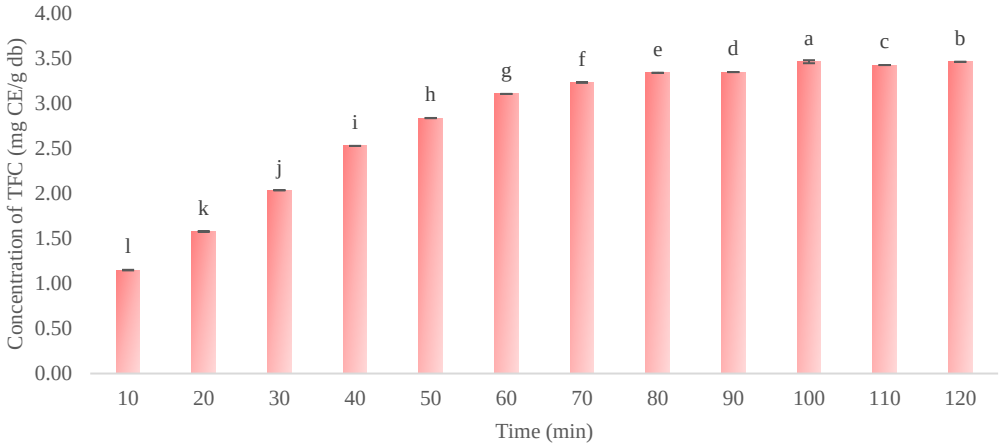

1:10

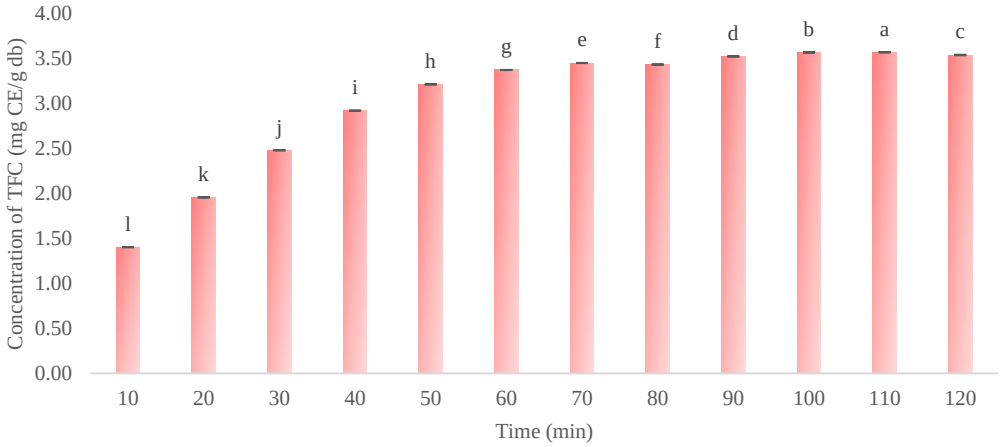

1:20

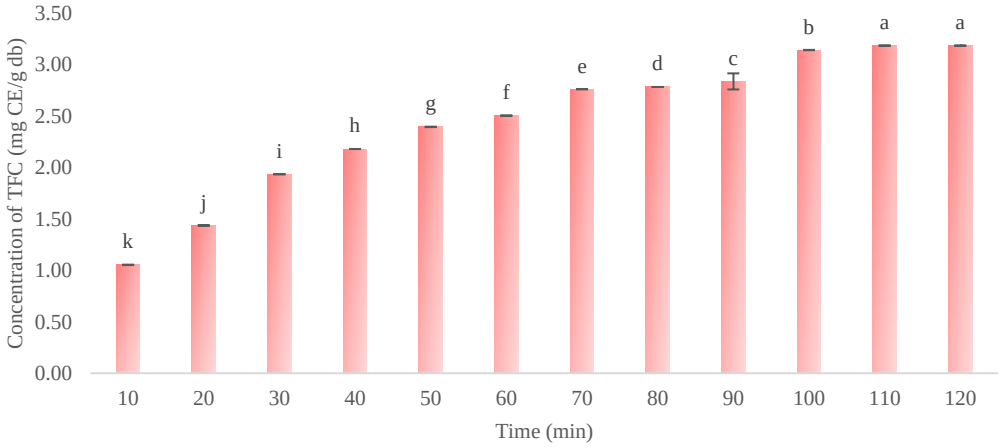

1:30

Figure 4 Concentrations of TFC in *M. citrifolia* fruits at different ratios over time. Values signify means ± standard deviations of three replicates. Distinct letters (within a bar) denote statistically significant differences (one-way ANOVA, Tukey's HSD test, $p < 0.05$).

To characterise the extraction kinetics of TFC in *M. citrifolia* fruits, six mathematical models were employed: the first-order kinetic, second-order kinetic, second-order rate, Peleg, power law, and two-site kinetic models. Figure 5 illustrates a comparison between the experimental and predicted extraction kinetics models for TFC at various ratios in *M. citrifolia* fruits. Subsequently, the results of fitting the

experimental data to the extraction kinetics models are presented in Table 2. Notably, the R^2 values ranged from 0.987 to 0.996 for the first-order kinetic model, 0.991 to 0.994 for the second-order kinetic model, 0.597 to 0.811 for the second-order rate model, 0.991 to 0.994 for the Peleg model, 0.958 to 0.990 for the power law model, and 0.995 to 0.997 for the two-site kinetic model. Additionally, R^2_{adj} values exhibited variations as follows: 0.085 to 0.096, 0.090 to 0.093, –0.344 to –0.108, 0.090 to 0.093, 0.054 to 0.089, and 0.094 to 0.097, respectively. RMSE values ranged from 0.024×10^{-1} to 0.063×10^{-1} for the first-order kinetic model, 0.028×10^{-1} to 0.054×10^{-1} for the second-order kinetic model, 0.716×10^{-1} to 1.699×10^{-1} for the second-order rate model, 0.028×10^{-1} to 0.054×10^{-1} for the Peleg model, 0.042×10^{-1} to 0.232×10^{-1} for the power law model, and 0.018×10^{-1} to 0.033×10^{-1} for the two-site kinetic law model. The lowest χ^2 values were recorded in the ranges of 0.020×10^{-4} to 0.316×10^{-4} for the first-order kinetic model, 0.001×10^{-4} to 0.033×10^{-4} for the second-order kinetic model, 0.000×10^{-4} for the second-order rate model, 0.001×10^{-4} to 0.033×10^{-4} for the Peleg model, 0.013×10^{-4} to 0.050×10^{-4} for the power law model, and 0.000×10^{-4} to 0.034×10^{-4} for the two-site kinetic model. MAE ranges were as follows: 0.398×10^{-2} to 1.272×10^{-2}, 0.088×10^{-2} to 0.411×10^{-2}, 0.000×10^{-2}, 0.088×10^{-2} to 0.411×10^{-2}, 0.258×10^{-2} to 0.576×10^{-2}, and 0.003×10^{-2} to 0.475×10^{-2} for the respective models.

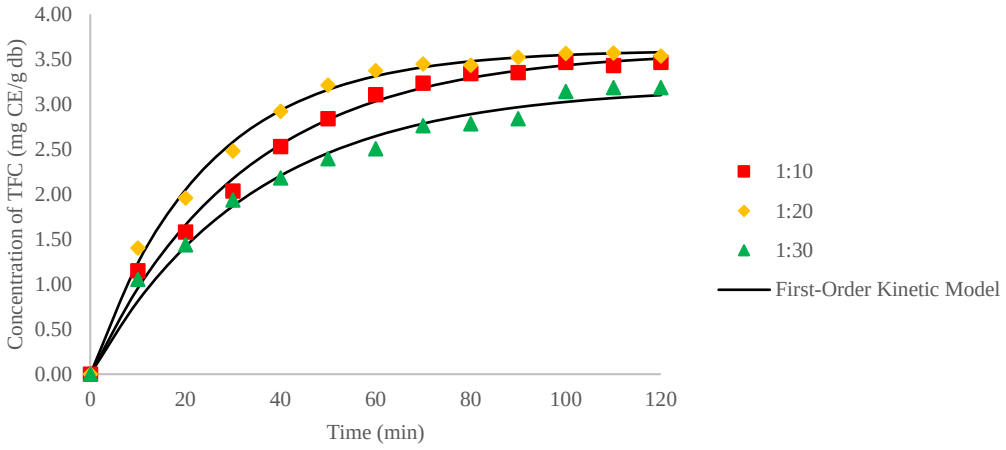

First-order kinetic

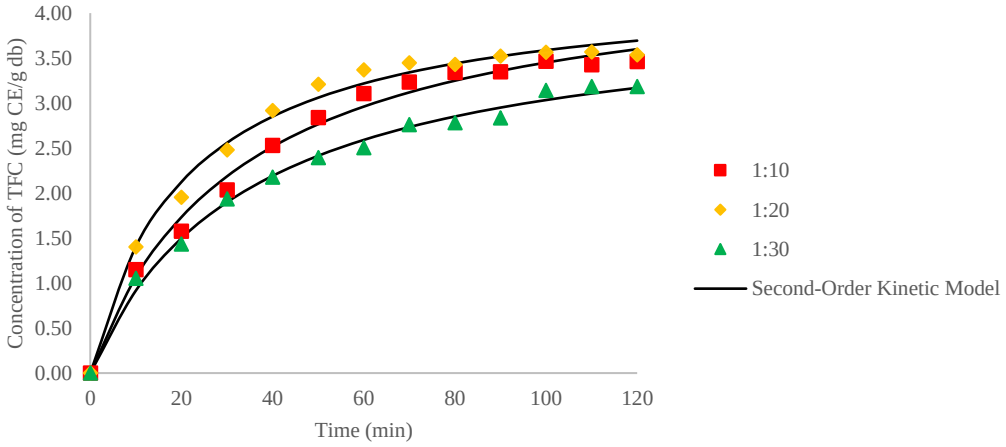

Second-order kinetic

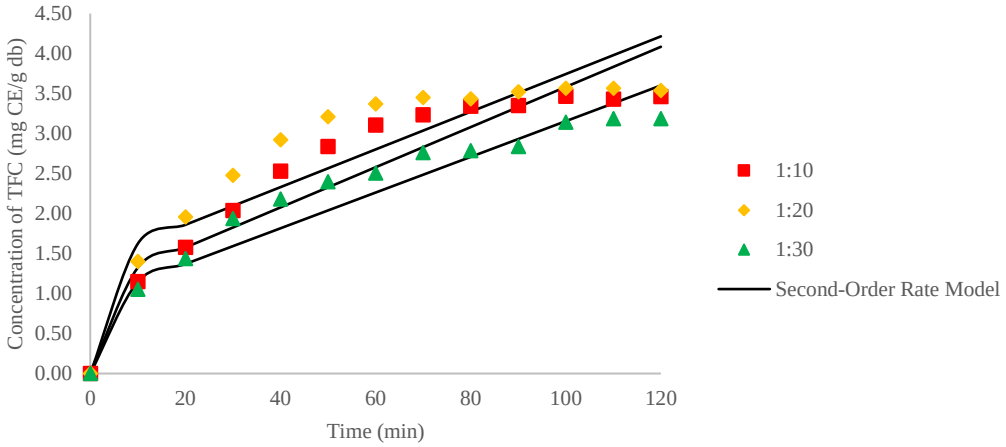

Second-order rate

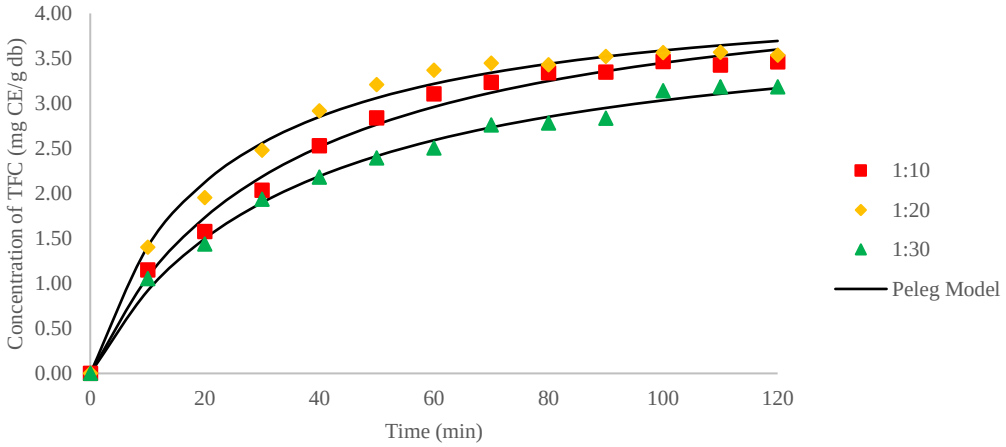

Peleg

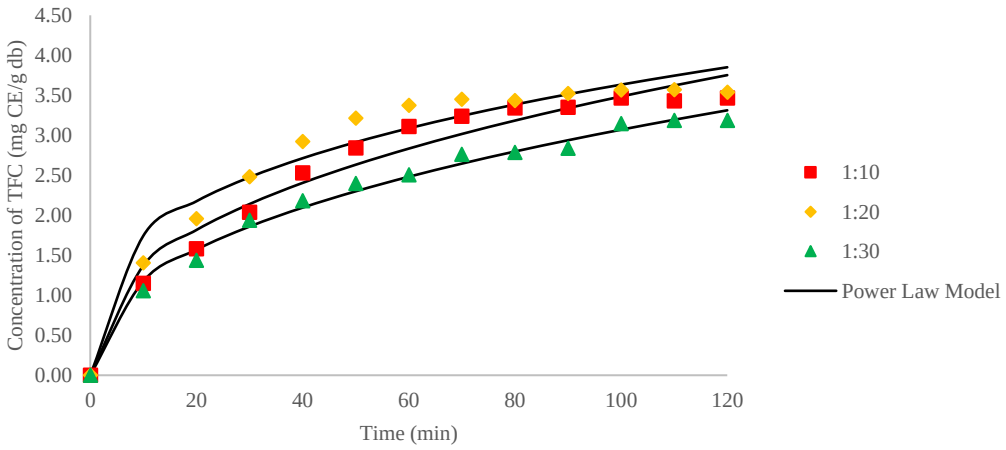

Power law

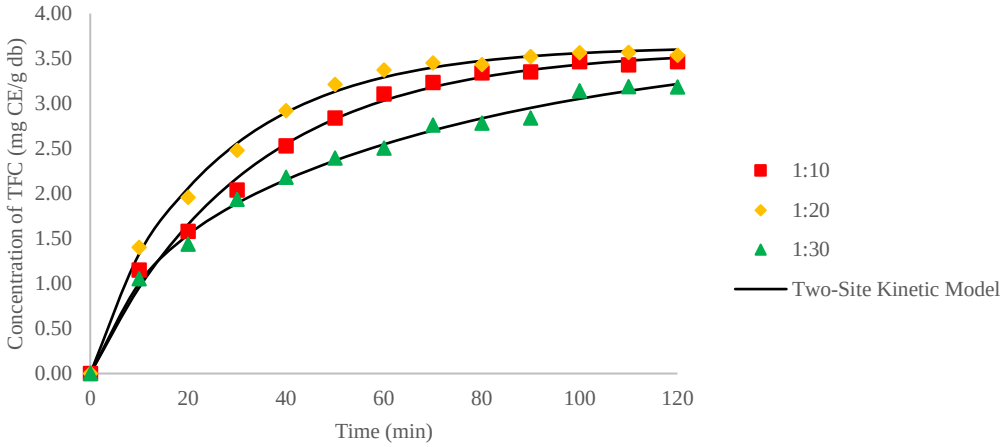

Two-site kinetic

Figure 5. Comparison of experimental and predicted data for the extraction kinetics models for TFC in *M. citrifolia* fruits at different ratios over time.

Table 2. Goodness of fit analysis for extraction kinetics models for TFC in *M. citrifolia* fruits at different ratios.

Model	Ratio	Constant	R^2	R^2_{adj}	RMSE (10^{-1})	χ^2 (10^{-4})	MAE (10^{-2})
First-order kinetic	1:10	C_e = 3.597	0.995	0.094	0.033	0.034	0.475
		k = 0.031					
	1:20	C_e = 3.602	0.996	0.096	0.024	0.020	0.398
		k = 0.042					
	1:30	C_e = 3.196	0.987	0.085	0.063	0.316	1.272
		k = 0.029					
Second-order kinetic	1:10	C_s = 4.588	0.991	0.090	0.054	0.001	0.088
		k = 0.007					
	1:20	C_s = 4.336	0.991	0.090	0.053	0.006	0.210
		k = 0.011					
	1:30	C_s = 4.081	0.994	0.093	0.028	0.033	0.411
		k = 0.007					
Second-order rate	1:10	h = 1.073	0.759	–0.165	1.153	0.000	0.000
		C_s = 39.842					
	1:20	h = 1.387	0.597	–0.344	1.699	0.000	0.000
		C_s = 42.440					
	1:30	h = 0.923	0.811	–0.108	0.716	0.000	0.000
		C_s = 44.809					
Peleg	1:10	k_1 = 7.186	0.991	0.090	0.054	0.001	0.088
		k_2 = 0.218					
	1:20	k_1 = 4.808	0.991	0.090	0.053	0.006	0.210
		k_2 = 0.231					
	1:30	k_1 = 8.459	0.994	0.093	0.028	0.033	0.411
		k_2 = 0.245					
Power law	1:10	B = 0.540	0.967	0.064	0.185	0.050	0.576
		n = 0.405					
	1:20	B = 0.837	0.958	0.054	0.232	0.027	0.462
		n = 0.319					
	1:30	B = 0.451	0.990	0.089	0.042	0.013	0.258
		n = 0.417					

Two-site kinetic	1:10	C_w = 2.505	0.995	0.094	0.033	0.034	0.475
		k_w = 0.031					
		C_d = 0.436					
		k_d = 0.031					
	1:20	C_w = 0.262	0.997	0.097	0.018	0.000	0.003
		k_w = 0.923					
		C_d = 12.851					
		k_d = 0.038					
	1:30	C_w = 1.001	0.995	0.095	0.021	0.001	0.057
		k_w = 0.104					
		C_d = 2.722					
		k_d = 0.014					

The two-site kinetic model exhibited the highest R^2 value at 1:20 (0.997), surpassing the values of 0.995 observed for both 1:10 and 1:30. This trend is consistent with the R^2_{adj} values. Additionally, the RMSE, χ^2, and MAE values for the two-site kinetic model were lower compared to other models. These results highlight the two-site kinetic model as a highly promising approach for characterising the extraction kinetics for TFC in *M. citrifolia* fruits at ratios of 1:10, 1:20, and 1:30, due to its exceptional fit. The trend in C_w values decreased from 1:10 (2.505 mg CE/g db) to 1:20 (0.262 mg CE/g db), followed by an increase at 1:30 (1.001 mg CE/g db). Conversely, the trend in C_d values increased from 1:10 (0.436 mg CE/g db) to 1:20 (12.851 mg CE/g db), then decreased at 1:30 (2.722 mg CE/g db). These fluctuations demonstrate how TFC concentrations varied across different ratios and stages due to extraction methods and fruit nature. The trend in k_w values fluctuated without a clear pattern, increasing from 1:10 (0.031 g db/mg CE·min) to 1:20 (0.923 g db/mg CE·min), then decreasing again at 1:30 (0.104 g db/mg CE·min). Similarly, the trend in k_d values also fluctuated, increasing from 1:10 (0.031 g db/mg CE·min) to 1:20 (0.038 g db/mg CE·min), then decreasing at 1:30 (0.014 g db/mg CE·min). These differences indicate a variability in the extraction rates during different stages and ratios, influenced by factors such as TFC solubility and extraction process efficiency. This provides crucial insights for optimising the extraction process to enhance both yield and efficiency.

Antioxidant Activity

The DPPH assay was employed to evaluate the antioxidant activity of *M. citrifolia* fruits, as depicted in Figure 6. The findings revealed a fluctuating trend in DPPH inhibition as the ratios gradually increased from 1:10 to 1:20, and then declined steadily to 1:30, with corresponding values ranging from 84.09 ± 0.01 % to 82.79 ± 0.01 %. Subsequently, *M. citrifolia* fruits extracted at 1:20 exhibited the highest DPPH inhibition, recorded at 88.39 ± 0.07 %. In contrast, the positive control demonstrated the highest inhibition rate at 90.02 ± 0.12 % for comparison. Notably, *M. citrifolia* fruits extracted at 1:20 displayed considerable potential for DPPH inhibition, indicating significant antioxidant activity.

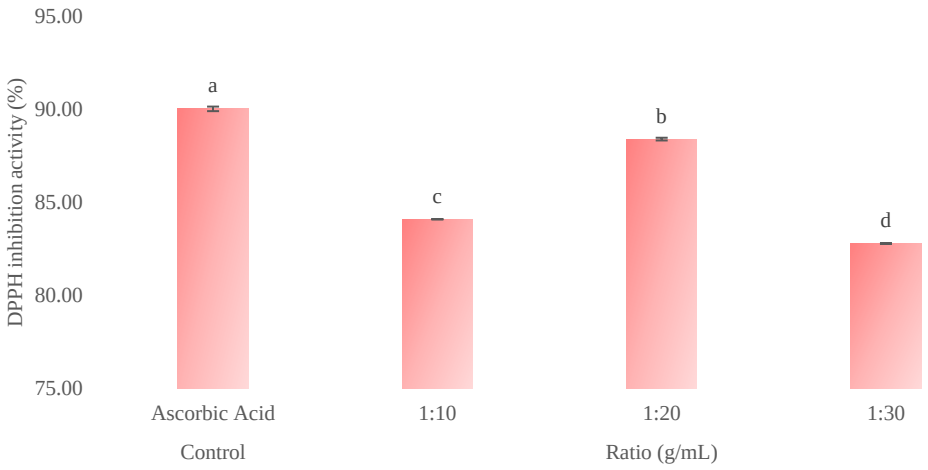

Figure 6. Assessment of antioxidant activity of *M. citrifolia* fruits using DPPH inhibition at different ratios. Values represent means ± standard deviations from three replicates. Different letters (within bars) indicate statistically significant differences (one-way ANOVA, Tukey's HSD test, $p < 0.05$). Ascorbic acid was used as a positive control.

DISCUSSION

The concentrations of yields in *M. citrifolia* fruits at various ratios over time, as illustrated in Figure 1, exhibited distinct patterns characterised by an initial sharp rise followed by stabilisation and peak yields, with slight variations among the ratios. Across all ratios studied, the 120-minute incubation period was found to achieve maximum yields. Notably, the 1:10 appeared to have a more pronounced effect on yield compared to 1:20 and 1:30. Figure 3 presents a unique pattern for TFC beyond the peak point under all conditions and different ratios. Specifically, at 100 min, TFC reached its peak at 1:10, while at 110 min and between 110–120 min, it recorded its highest values at 1:20 and 1:30, respectively. Overall, the highest ratio, 1:20, exhibited superior performance compared to other ratios. This phenomenon is attributed to the larger contact area resulting from the 1:10 affecting yield and the 1:20 influencing TFC, facilitating more effective dissolution of substances and enhancing extraction yields [23,24]. Several studies support the notion that a lower volume of solvent relative to plant material leads to higher yields of bioactive compounds. For instance, Do et al. [25] found that a lower solvent-to-sample ratio yielded the greatest phenolic and flavonoid contents from *Limnophila aromatica*. Additionally, Liao et al. [26] observed no significant change in extraction yields as ratios increased from 40 to 70 mL/g. This suggests that beyond a certain point, increasing the solvent ratio does not proportionally increase the extract yield. In general, increasing the ratio enhances the extraction of *M. citrifolia* fruits until a specific threshold is reached, which was 1:10 for yield and 1:20 for TFC. Beyond this threshold, further increases in the ratio lead to diminishing yields, which could be due to either the saturation of the solid-to-liquid ratio or the degradation of plant material. Moreover, if there is a reduction in yield, as noted earlier, it may impact the overall efficiency of the extraction process and influence how yield is modelled in extraction kinetics. Nevertheless, these observations primarily reflect thermal degradation rates rather than genuine kinetics [27].

While the utilisation of ratios as variables in mathematical modelling for extraction kinetics remains relatively unexplored, evidence suggests that the two-site kinetic model has shown remarkable success. Meziane and Kadi [28] conducted research on the extraction kinetics of oil from olive cake using 96 % ethanol at various solvent-to-solid ratios and temperatures. Their study also delved into the thermodynamics of the process. The kinetics analysis revealed that the results obtained from the two-site kinetic model exhibited a high degree of agreement with experimental data. The oil yield increased with yield of bioactive compounds. Moreover, the use of an ultrasonic water bath may be limited in its ability to efficiently extract compounds from plant material prolonged contact time, higher solvent-to-solids ratios, and elevated extraction temperatures. Additionally, mass transfer coefficients were determined for the solid-to-liquid ratio and temperature at different extraction stages, indicating a linear increase for both parameters. The research concluded that the oil washing out from particle surfaces was primarily responsible for all forms of extractions. Similarly, Tao et al. [29] emphasised the impact of particle size and solvent nature on extraction kinetics, recommending the two-site kinetic model as the most suitable. These studies provide substantial support for the application of the two-site kinetic theory in extraction kinetics involving solid-to-liquid ratios. Hence, these findings reaffirm the suitability of the two-site kinetic model as an effective tool for analysing complexities of solid-liquid extractions.

Antioxidants play a crucial role in reducing oxidative stress and preventing diseases. They are often assessed by measuring the reduction of the DPPH free radical scavenging activity, resulting in a change of colour and reduced absorbance at 517 nm [30]. In this study, 1:20 emerged as the most effective extraction method for DPPH inhibition in *M. citrifolia* fruits. However, there is limited research on the use of fruits in various solid-to-liquid ratios to enhance antioxidant activity. A study by Samaram et al. [31] found that the DPPH free radical scavenging activity of papaya seeds was maximised at a ratio of 1:7 (w/v) within the range of 1:6 to 1:10, suggesting that a lower ratio enhanced antioxidant capacity. Additionally, flavonoids, a class of polyphenolic compounds renowned for their potent antioxidative properties, play a crucial role in neutralising reactive oxygen species and mitigating oxidative damage. The presence of flavonoids in *M. citrifolia* is associated with its antioxidant capabilities. Optimising the extraction ratio at 1:20 could enhance the flavonoid concentration as well as the antioxidant capacity of *M. citrifolia* fruits. With elevated flavonoid concentrations, this underutilised fruit can contribute to products that offer additional health benefits, such as improved antioxidant status and potential protection against chronic diseases, making them ideal candidates for developing functional foods. Therefore, these findings have the potential to augment the nutritional and therapeutic value of *M. citrifolia* fruits.

While the study offers comprehensive findings on the extraction kinetics and antioxidant activity of *M. citrifolia* fruits, several limitations were encountered during experimentation. The choice of solvent is critical as it can impact the solubility of flavonoid compounds in *M. citrifolia* fruits. Different solvents possess varying polarities and extraction efficiencies, potentially leading to variations in the due to inadequate agitation and penetration. While ultrasonic waves can disrupt cell walls and aid in extraction, their effectiveness may be constrained by

factors such as the density and structure of the plant material. Lastly, the assumptions regarding antioxidant concentrations determined solely through the DPPH assay require further validation using other assays such as oxygen radical absorbance capacity, while the mechanism of action should be further validated through in vitro and in vivo studies.

CONCLUSION

The highest yield and TFC values for *M. citrifolia* fruits were observed with solid-to-liquid ratios of 1:10 and 1:20, at 1.46 ± 0.00 mg/mL and 3.57 ± 0.00 mg CE/g db, respectively, reaching an optimum level to enhance the yield and TFC of *M. citrifolia* fruits. The two-site kinetic model effectively elucidated the extraction kinetics of both yield and TFC. The DPPH inhibition also indicated noteworthy antioxidant effects, with the highest value of 88.39 ± 0.07 % recorded at 1:20. This finding highlights the potential for developing standardised extraction kinetics for *M. citrifolia* fruits based on solid-to-liquid ratios, offering potential benefits in terms of cost savings and time for the food and pharmaceutical industries.

Future research could explore alternative extraction methods, investigate the impact of additional variables such as temperature and pH, and conduct in-depth mechanistic studies to elucidate the underlying extraction mechanisms, thereby enhancing understanding and optimising the extraction process of *M. citrifolia* fruits. Furthermore, additional parameters and mechanisms involved in this extraction process, such as acoustic energy density, temperature variations, and solute distribution patterns, must be considered for accurately simulating extraction processes.

ACKNOWLEDGEMENTS

The authors extend their gratitude to the Faculty of Food Science and Nutrition, Universiti Malaysia Sabah, for their financial support. This research was supported by Universiti Malaysia Sabah from Skim Pensyarah Lantikan Baru (SLB2234).

REFERENCES

1. Abd Aziz, N. A., Hasham, R., Sarmidi, M. R., Suhaimi, S. H. & Idris, M. K. H. (2021) A review on extraction techniques and therapeutic value of polar bioactives from Asian medicinal herbs: Case study on *Orthosiphon aristatus*, *Eurycoma longifolia* and *Andrographis paniculata*. *Saudi Pharmaceutical Journal*, **29**, 143–165. https://doi.org/10.1016/j.jsps.2020.12.016

2. Kurek, M., Benaida-Debbache, N., Garofulić, I. E., Galić, K., Avallone, S., Voilley, A. & Waché, Y. (2022) Antioxidants and bioactive compounds in food: Critical review of issues and prospects †. *Antioxidants*, **11**, 742. https://doi.org/10.3390/antiox11040742

3. Bolouri, P., Salami, R., Kouhi, S., Kordi, M., Asgari Lajayer, B., Hadian, J. & Astatkie, T. (2022) Applications of essential oils and plant extracts in different industries. *Molecules*, **27**, 8999. https://doi.org/10.3390/molecules27248999

4. Ha, G.-S. & Kim, J.-H. (2016) Kinetic and thermodynamic characteristics of ultrasound-assisted extraction for recovery of paclitaxel from biomass. *Process Biochemistry*, **51**, 1664–1673. https://doi.org/10.1016/j.procbio.2016.08.012

5. Patil, D. M. & Akamanchi, K. G. (2017) Ultrasound-assisted rapid extraction and kinetic modelling of influential factors: Extraction of camptothecin from *Nothapodytes nimmoniana* plant. *Ultrasonics Sonochemistry*, **37**, 582–591. https://doi.org/10.1016/j.ultsonch.2017.02.015

6. Deng, S., West, B. J. & Jensen, C. J. (2010) A quantitative comparison of phytochemical components in global Noni fruits and their commercial products. *Food Chemistry*, **122**, 267–270. https://doi.org/10.1016/j.foodchem.2010.01.031

7. Almeida, É. S., de Oliveira, D. & Hotza, D. (2019) Properties and applications of *Morinda citrifolia* (Noni): A review. *Comprehensive Reviews in Food Science and Food Safety*, **18**, 883–909. https://doi.org/10.1111/1541-4337.12456

8. Abou Assi, R., Darwis, Y., Abdulbaqi, I. M., khan, A. A., Vuanghao, L. & Laghari, M. H. (2017) *Morinda citrifolia* (Noni): A comprehensive review on its industrial uses, pharmacological activities, and clinical trials. *Arabian Journal of Chemistry*, **10**, 691–707. https://doi.org/10.1016/j.arabjc.2015.06.018

9. European Commission (2010) Commission Decision of 21 April 2010 authorising the placing on the market of puree and concentrate of the fruits of *Morinda citrifolia* as a novel food ingredient under Regulation (EC) No 258/97 of the European Parliament and of the Council. *Official Journal of the European Union*, **102**, 49–51.

10. Panche, A. N., Diwan, A. D. & Chandra, S. R. (2016) Flavonoids: An overview. *Journal of Nutritional Science*, **5**, e47. https://doi.org/10.1017/jns.2016.41

11. Sam-ang, P., Phanumartwiwath, A., Liana, D., Sureram, S., Hongmanee, P. & Kittakoop, P. (2023) UHPLC-QQQ-MS and RP-HPLC detection of bioactive alizarin and scopoletin metabolites

from *Morinda citrifolia* root extracts and their antitubercular, antibacterial, and antioxidant activities. *ACS Omega*, **8**, 29615–29624. https://doi.org/10.1021/acsomega.3c03656

12. Ali, M., Kenganora, M. & Manjula, S. N. (2016) Health benefits of *Morinda citrifolia* (Noni): A review. *Pharmacognosy Journal*, **8**, 321–334. https://doi.org/10.5530/pj.2016.4.4

13. Stephenus, F. N., Benjamin, M. A. Z., Anuar, A. & Awang, M. A. (2023) Effect of temperatures on drying kinetics, extraction yield, phenolics, flavonoids, and antioxidant activity of *Phaleria macrocarpa* (Scheff.) Boerl. (Mahkota Dewa) fruits. *Foods*, **12**, 2859. https://doi.org/10.3390/foods12152859

14. Lin, C. B., Poh, J. & Ali, A. (2018) Extraction kinetic of *Ziziphus jujuba* fruit using solid-liquid extraction. *Journal of Engineering Science and Technology*, **13**, 27–39.

15. Awang, M. A., Daud, N. N. N. N. M., Ismail, N. I. M., Cheng, P. G., Ismail, M. F. & Ramaiya, S. D. (2021) Antioxidant and cytotoxicity activity of *Cordyceps militaris* extracts against human colorectal cancer cell line. *Journal of Applied Pharmaceutical Science*, **11**, 105–109. https://doi.org/10.7324/JAPS.2021.110711

16. Hobbi, P., Okoro, O. V., Delporte, C., Alimoradi, H., Podstawczyk, D., Nie, L., Bernaerts, K. V. & Shavandi, A. (2021) Kinetic modelling of the solid–liquid extraction process of polyphenolic compounds from apple pomace: Influence of solvent composition and temperature. *Bioresources and Bioprocessing*, **8**, 114. https://doi.org/10.1186/s40643-021-00465-4

17. Rakshit, M., Srivastav, P. P. & Bhunia, K. (2020) Kinetic modeling of ultrasonic-assisted extraction of punicalagin from pomegranate peel. *Journal of Food Process Engineering*, **43**, e13533. https://doi.org/10.1111/jfpe.13533

18. Natolino, A. & Da Porto, C. (2020) Kinetic models for conventional and ultrasound assistant extraction of polyphenols from defatted fresh and distilled grape marc and its main components skins and seeds. *Chemical Engineering Research and Design*, **156**, 1–12. https://doi.org/10.1016/j.cherd.2020.01.009

19. Peleg, M. (1988) An empirical model for the description of moisture sorption curves. *Journal of Food Science*, **53**, 1216–1217. https://doi.org/10.1111/j.1365-2621.1988.tb13565.x

20. Dong, Z., Gu, F., Xu, F. & Wang, Q. (2014) Comparison of four kinds of extraction techniques and kinetics of microwave-assisted extraction of vanillin from *Vanilla planifolia* Andrews. *Food Chemistry*, **149**, 54–61. https://doi.org/10.1016/j.foodchem.2013.10.052

21. So, G. C. & Macdonald, D. G. (1986) Kinetics of oil extraction from canola (rapeseed). *The Canadian Journal of Chemical Engineering*, **64**, 80–86. https://doi.org/10.1002/cjce.5450640112

22. Awang, M. A., Benjamin, M. A. Z., Anuar, A., Ismail, M. F., Ramaiya, S. D. & Mohd Hashim, S. N. A. (2023) Dataset of gallic acid quantification and their antioxidant and anti-inflammatory activities of different solvent extractions from Kacip Fatimah (*Labisia pumila* Benth. & Hook. f.) leaves. *Data in Brief*, **51**, 109644. https://doi.org/10.1016/j.dib.2023.109644

23. Xie, G., Li, R., Han, Y., Zhu, Y., Wu, G. & Qin, M. (2017) Optimization of the extraction conditions for *Buddleja officinalis* Maxim. using response surface methodology and exploration of the optimum harvest time. *Molecules*, **22**, 1877. https://doi.org/10.3390/molecules22111877

24. Andres, A. I., Petron, M. J., Lopez, A. M. & Timon, M. L. (2020) Optimization of extraction conditions to improve phenolic content and in vitro antioxidant activity in craft brewers' spent grain using response surface methodology (RSM). *Foods*, **9**, 1398. https://doi.org/10.3390/foods9101398

25. Do, Q. D., Angkawijaya, A. E., Tran-Nguyen, P. L., Huynh, L. H., Soetaredjo, F. E., Ismadji, S. & Ju, Y.-H. (2014) Effect of extraction solvent on total phenol content, total flavonoid content, and antioxidant activity of *Limnophila aromatica*. *Journal of Food and Drug Analysis*, **22**, 296–302. https://doi.org/10.1016/j.jfda.2013.11.001

26. Liao, J., Qu, B. & Zheng, N. (2016) Effects of process parameters on the extraction of quercetin and rutin from the stalks of *Euonymus alatus* (Thumb.) Sieb and predictive model based on least squares support vector machine optimized by an improved fruit fly optimization algorithm. *Applied Sciences*, **6**, 340. https://doi.org/10.3390/ app6110340

27. Chemat, F., Rombaut, N., Sicaire, A.-G., Meullemiestre, A., Fabiano-Tixier, A.-S. & Abert-Vian, M. (2017) Ultrasound assisted extraction of food and natural products. Mechanisms, techniques, combinations, protocols and applications. A review. *Ultrasonics Sonochemistry*, **34**, 540–560. https://doi.org/10.1016/j.ultsonch.2016.06.035

28. Meziane, S. & Kadi, H. (2008) Kinetics and thermodynamics of oil extraction from olive

cake. *Journal of the American Oil Chemists' Society*, **85**, 391–396. https://doi.org/10.1007/s11746-008-1205-2

29. Tao, Y., Zhang, Z. & Sun, D.-W. (2014) Kinetic modeling of ultrasound-assisted extraction of phenolic compounds from grape marc: Influence of acoustic energy density and temperature. *Ultrasonics Sonochemistry*, **21**, 1461–1469. https://doi.org/10.1016/j.ultsonch.2014.01.029

30. Moon, J.-K. & Shibamoto, T. (2009) Antioxidant assays for plant and food components. *Journal of Agricultural and Food Chemistry*, **57**, 1655–1666. https://doi.org/10.1021/jf803537k

31. Samaram, S., Mirhosseini, H., Tan, C. P., Ghazali, H. M., Bordbar, S., Serjouie, A. & Anlı, R. E. (2015) Optimisation of ultrasound-assisted extraction of oil from papaya seed by response surface methodology: Oil recovery, radical scavenging antioxidant activity, and oxidation stability. *Food Chemistry*, **172**, 7–17. https://doi.org/ 10.1016/j.foodchem.2014.08.068